Monthly Notices of the ROYAL ASTRONOMICAL SOCIETY
MNRAS **509,** L17–L20 (2022) https://doi.org/10.1093/mnrasl/slab115
Advance Access publication 2021 October 25

Comparison of the mass distributions of short-period exoplanets detected by transit and RV methods

Oleg Ya. Yakovlev,[1★] V. I. Ananyeva,[1] A. E. Ivanova[1,2] and A. V. Tavrov[1,3]
[1]*Space Research Institute, Russian Academy of Sciences, 84/32 Profsoyuznaya Str, Moscow 117997, Russia*
[2]*LATMOS-IPSL, 78280 Guyancourt, France*
[3]*Moscow Institute of Physics and Technology, Dolgoprudnii, Moscow oblast 141701, Russia*

Accepted 2021 October 13. Received 2021 October 12; in original form 2021 August 12

ABSTRACT
We analyse the causes of a discrepancy between the earlier obtained samples of the mass distributions of exoplanets detected by the transit method and the radial velocity (RV) one and corrected for some observational selection effects. It is found that this discrepancy can be removed by introducing the following restrictions into the procedures forming the samples: (i) to consider, among transit exoplanets, only those which masses were determined by the RV method (i.e. excluding the transit time variation method); (ii) to take into account exoplanets with orbital periods $P \in [1, 100]$ days and masses $M \in [0.02, 13]M_J$ (Jupiter masses). In addition, we compare here the distributions by projective masses (which is $M\sin i$, where i is the orbital inclination of an exoplanet). For this, the mass distribution of transit exoplanets is transformed into the projective mass distribution. Due to these three changes in the procedure, the obtained RV and transit distributions exhibit a similar behaviour in an interval of $M \in [0.02, M_{\mathrm{mid}}]M_J$ and coincide at $M \in [M_{\mathrm{mid}}, 13]M_J$, where $M_{mid} \approx 0.17M_J$.

Key words: methods: observational, statistical – techniques: photometric, radial velocities – planets and satellites: fundamental parameters.

1 INTRODUCTION

Statistical studies in exoplanetary science are important for estimating the abundance of planets of different types and for comparing with the models of planetary formation and evolution. However, the mass distribution of discovered exoplanets is strongly biased by various factors of observational selection caused by peculiarities in the observational methods [methods of transits, radial velocities (RVs), etc.] and observational programs.

Earlier, we obtained two independent mass distributions for exoplanets discovered by the *Kepler Space Telescope* by the transit method (Ananyeva et al. 2020) (A20 hereafter) and those discovered by the RV method (Ivanova et al. 2021) (I20 hereafter). Several important observational selection factors were taken into account in both cases.

A20 considered the distribution of transit exoplanets corrected by accounting for the transit probability (Petigura, Howard & Marcy 2013) and the probability of mass determination through the weight coefficients k_1 and k, respectively. The coefficient k_1 is defined as the ratio of the semi-major axis of the exoplanet's orbit a to the radius of the host star r: $k_1 = a/r$ (Winn 2011). The coefficient k is the fraction of detected transit exoplanets which mass could be determined by RV method to the total of transit detected planets, in each bin of their radius R (A20). They approximated this distribution by a power law $\frac{\partial N}{\partial M} \propto M^{-\alpha}$ with an exponent $\alpha = -2$ over the entire investigated interval.

★ E-mail: yko-v@yandex.ru

I20 took into account the probability of detecting an exoplanet by the method of RV from its mass M and orbital period P. The distribution law for the projective mass $M_{\mathrm{pr}} \equiv M\sin i$ (i is the inclination of the exoplanet's orbit) was obtained, which is qualitatively close to a broken power law with an exponents $\alpha \approx -1$ and -2 in the middle mass interval $M \in [0.14, 2]M_J$ and in the outer intervals ([0.011, 0.14], [2, 13]M_J), respectively. These distributions are shown in Fig. 1, where the quantity 'Norm Fraction' laid off as ordinate corresponds to the distribution in masses or projective masses depending on the curves, which are normalized to unity.

As compared to the distribution of transit exoplanets, the distribution of the RV exoplanets exhibits a lack of exoplanets in the interval of small masses and, in particular, a local minimum at $M \approx 0.1\ M_J$. In addition, there is a lack of transiting exoplanets in the range of giant planets ($M > 2\ M_J$). The aim of this paper is to explain the differences in the mass distributions of transit and RV exoplanets. We use the data about exoplanets from the NASA Exoplanet Archive as on March 2021.

2 ADDITIONAL RESTRICTIONS ON THE SAMPLINGS

When comparing the mass distributions of transit and RV exoplanets, it is the difference in the considered ranges of their orbital periods P and masses M that should be taken into account in the first place. The transit method detected exoplanets with a period of $P < 1110$ d (by the *Kepler Space Telescope*); and for most of them (95 per cent), $P < 100$ d (Fig. 2). For the distribution of transit exoplanets (A20), no restrictions on the period were introduced; and a mass range of

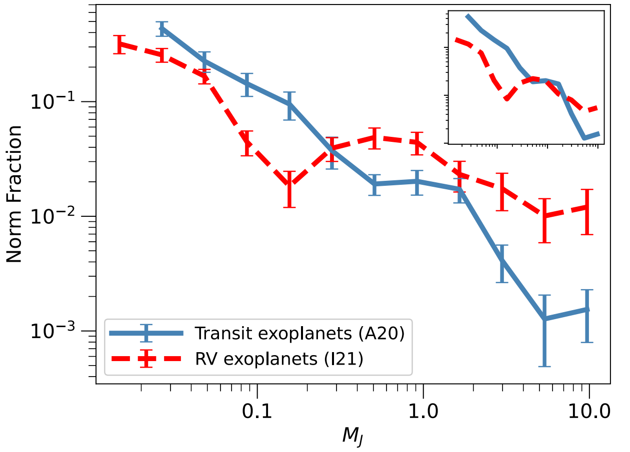

Figure 1. The distribution of RV exoplanets versus projective masses $\frac{\partial N}{\partial M_{\rm pr}}$ (dashed red line) from I21 (the period is $P \in [1, 100]$ d for $M \in [0.011, 13]M_{\rm J}$) and the distribution of transit exoplanets versus mass $\frac{\partial N}{\partial M}$ for $M \in [0.02, 13]M_{\rm J}$ from A20 (blue line; transit planets detected by the *Kepler Space Telescope* are taken into account). In the inset, the same distributions (on the same scale) normalized to the interval centred at $M \approx 0.92\ M_{\rm J}$.

$[0.02, 13]M_{\rm J}$ was considered. At the same time, 95 per cent of RV exoplanets were found with a period of $P < 4500$ d; and only for 37 per cent of them, $P < 100$ d. In the distribution of RV exoplanets (I20), exoplanets with masses $M \in [0.011, 13]M_{\rm J}$ and periods $P \in [1, 100]$ days were considered. In this work, we take into account transit and RV exoplanets only with periods $P \in [1, 100]$ d in the mass range $M \in [0.02, 13]M_{\rm J}$ for comparing mass distributions.

The masses of transit exoplanets were determined by the RV method and the TTV method. The selectivity of determining the mass by the RV method is expressed by the relative increase in the observed number of heavier exoplanets of known masses. To take this factor into account, the mass determination coefficient $k = f(R)$ was introduced in A20. As a hypothesis explaining the excess of transit exoplanets in a mass interval of $M < 0.4M_{\rm J}$, we consider the contribution to the distribution of transit exoplanets, the masses of which were determined by the TTV method. The selectivity of the latter is inverse: 88 per cent of the TTV exoplanets have a mass of $M < 0.21M_{\rm J}$ (Fig. 2). Moreover, in the interval $M \in [0.05, 0.2]M_{\rm J}$, the TTV method yielded the masses for twice as many planets as the RV method (33 planets versus 16 ones with $M \in [0.087, 0.21]M_{\rm J}$); and for large masses, a portion of planets with masses determined with the TTV method sharply decreases to zero at $M > 2M_{\rm J}$.

The TTV method is based on the analysis of variations in the onset of transits caused by the gravitational interaction of planets with each other. The mutual gravitational influence of the planets becomes especially noticeable if they are close to a low-order orbital resonance, i.e. if their orbital periods relate to each other as small integers (2:1, 3:2, 3:1, etc.). However, with the TTV method, the 'nominal' masses rather than the true ones are determined (Hadden & Lithwick 2013). The difference between the true and nominal masses grows with increasing the eccentricities of the orbits of exoplanets, being in orbital resonance; and this difference may reach a factor of 2–3 for eccentricities of 0.01–0.03. If the RVs of the parent star are not available, the observations of transits alone cannot help to measure such small orbital eccentricities and to determine reliably the true masses of exoplanets instead of the nominal ones.

As is seen from Fig. 2b, in the mass-radius plane below the iron curve, which corresponds to the dependence of the radius on the mass for an iron planet (Fortney et al. 2007), there are exoplanets

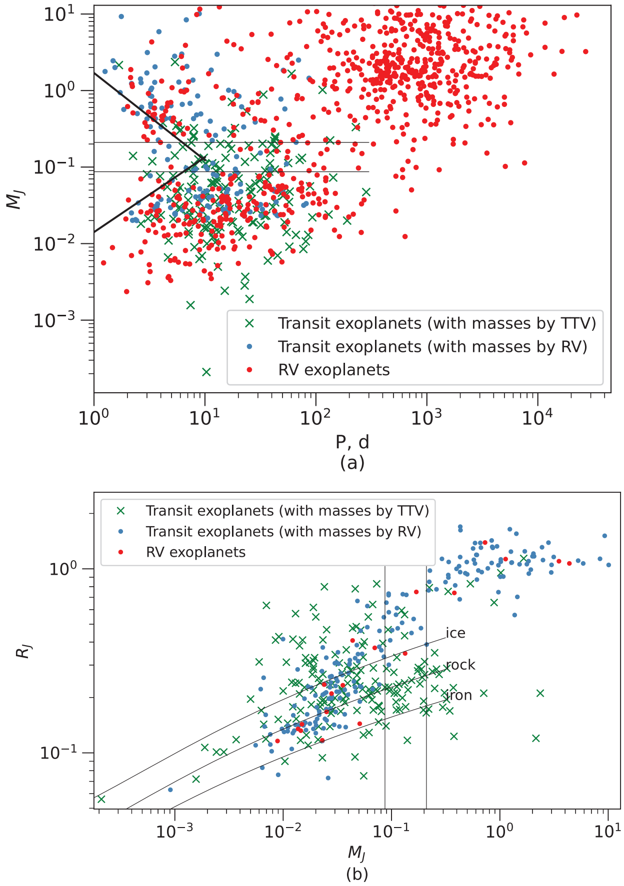

Figure 2. Exoplanets in the period-mass (a) and mass-radius (b) planes. The transit exoplanets are shown by green and blue symbols and RV exoplanets are shown by red symbols (the radius is known only for 19 RV exoplanets). The x-symbols show exoplanets, the masses of which were determined by the transit time variation (TTV) method. The black curves labelled as 'ice', 'rock', and 'iron' are the theoretical radius-versus-mass dependencies for icy, rocky, and iron planets (Fortney, Marley & Barnes 2007). The horizontal [in panel (a)] and vertical [in panel (b)] lines mark the mass interval $[0.087, 0.21]M_{\rm J}$, in which there is a minimum in the mass distributions of exoplanets. In panel (a), the area of the hot Neptunian desert is shown (Mazeh, Holczer & Faigler 2016).

with a very high density. Their masses, except that of Kepler-131 c, were determined by the TTV method. Iron is the densest chemical element among those frequently occurring in the Galaxy and determining the composition of planets. Consequently, due to physical reasons, planets with an average density higher than that of iron planets (below the iron curve) can hardly exist. Since the true masses of transit exoplanets cannot be determined with the TTV method, we compare below the distributions only for exoplanets which masses were determined with the RV method. 217 RV and 147 transit exoplanets remain for analysis due to the introduced restrictions.

3 COMPARISON OF DISTRIBUTIONS

For RV exoplanets, the projective mass ($M_{\rm pr}$) is known. In order to compare the mass distributions of transit and RV exoplanets, the distribution of transit exoplanets by true masses is converted into the distribution versus projective masses $M_{\rm pr}$. (It is easier to perform this conversion than to transform the distribution of RV exoplanets

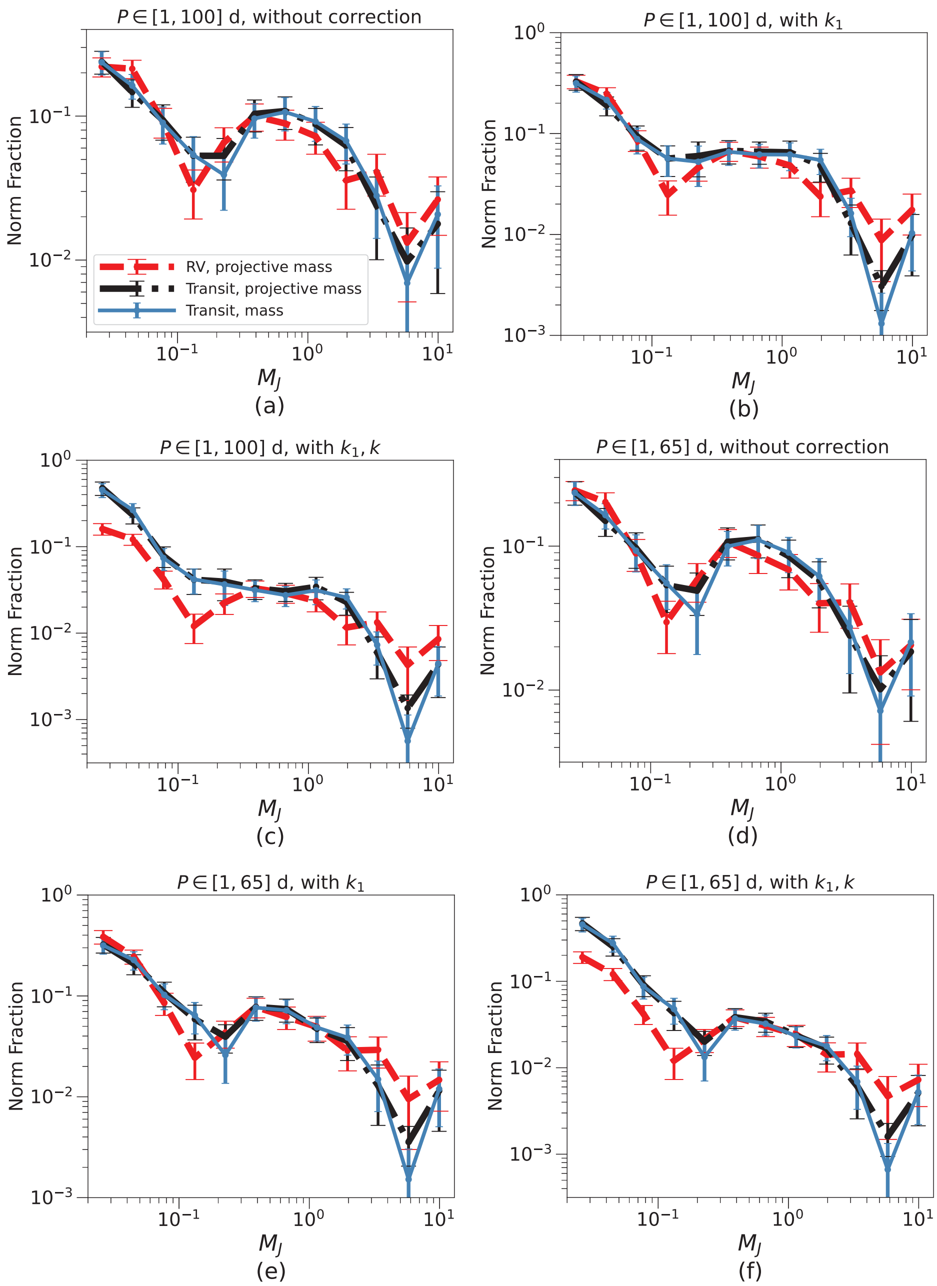

Figure 3. The projective mass distributions for exoplanets detected by the RV and transit methods, and the mass distributions for transit exoplanets [see the legend in panel (a)]. Panels (a)–(c) and (d)–(f) present the planets with orbital periods $P \in [1, 100]$ and $P \in [1, 65]$ days, respectively. The distributions without correction are in panels (a) and (d). The distributions for transit exoplanets are corrected with the transit probability coefficient k_1 [panels (b) and (e)] and additionally with the mass determination coefficient k [panels (c) and (f)]. The distribution for RV exoplanets are corrected according to I20 [(panels (b), (c), (e), and (f)]. The distributions in these panels [except (a), (b)] are normalized to the value in the central bin. Only transit exoplanets which masses were determined by the RV method are considered here.

versus projective masses to that versus true masses). For this, in each of the distribution histogram bins, we determine a weight coefficient, which is proportional to the probability of the projective mass M_{pr} of the exoplanet in this bin. This probability P is defined according to the distribution function of the random variable $\sin i$: $P(\sin i < Z) = 1 - \cos \arcsin Z$, where $Z \in [0, 1]$ (Ho & Turner 2011). In this case, we also consider objects with $M > 13M_J$ (for one object, $M = 18M_J$), which contribute to the distribution over projective masses M_{pr}.

Fig. 3 shows the considered distributions before and after the correction accounting for the observational selection (for the factors presented in the Introduction). The correction techniques were described in detail by Ivanova et al. (2019), A20, and Yakovlev et al. (2021) for transit exoplanets and by I20 for RV exoplanets with the restrictions introduced in the previous section.

For transit exoplanets, the conversion from the true masses (black curves in Fig. 3) to the projective masses (blue curves) diminishes the depth of the minima in the distributions, while their slopes change only in the regions close to the minima. For all distributions in Fig. 3, a minimum is visible in the interval of giant planets at $M \approx 7.5\ M_J$. The minimum in an interval of $M \in [0.1, 0.3]M_J$ of various depths is also present in all of the distributions, except for the corrected transit distributions with periods $P \in [1, 100]$ d. (Figs 3b and c). This exception is caused by the presence of exoplanet Kepler-413 b in the 5th bin with a period of 66 days, the transit probability of which is small (7 times less than the median value for other 8 exoplanets from this bin with periods $P < 65$ d). This planet has a significant impact on the distribution in an interval of $M \in [0.17, 0.3]M_{\rm J}$, due to which the minimum is smoothed out. The latter can be observed when this planet is removed from the consideration (Figs 3 d–f for $P \in [1, 65]$ d) with other exoplanets with periods $P \in [65, 100]$ d. There are 23 RV and 5 transit exoplanets in range $P \in [65, 100]$ d. This minimum is explained by a lack of Neptune-like exoplanets with a period of $P < 10$ d ('the hot Neptunian desert', see Fig. 2), which is caused by photoevaporation of the atmospheres of exoplanets of this type by the influence of radiation from the star (Mazeh et al. 2016).

The transit and RV distributions versus projective masses in Figs 3 a and d, for which the observational selection factors are ignored, coincide with each other in the entire considered mass interval (within the uncertainty). The corresponding distributions also coincide when the transit probability is taken into account for transit exoplanets (Figs 3 b and e), except interval with minimum at M $0.1M_{\rm J}$. When the mass determination coefficient k is additionally accounted for (Figs 3 c and f), in the low-mass range, where the distribution slopes for transit and RV exoplanets are close (they both follow to power law $\frac{\partial N}{\partial M} \propto M^{-\alpha}$ with $\alpha \approx -3$, which match on these mass range to semitheoretical law in Emsenhuber et al. (2020)), the transit and RV projective mass distributions disagree.

The two-samples Kolmogorov–Smirnov test was carried out for these 6 cases (shown in the panels in Fig. 3) with a significance level $\alpha = 0.05$. According to this test, the hypothesis of the correspondence between the projective mass distributions of RV and transit exoplanets was confirmed for cases a, b on the entire mass range and for cases b, e, f on the mass range $M \in [0.17, 13]M_{\rm J}$.

This probably suggests that the number of low-mass planets detected by the RV method is underestimated. Planets with small masses induce fluctuations in the RV of a parent star (1–2 $\rm m\,s^{-1}$ or less), the amplitude of which is low and comparable to the error of a single measurement of the star's RV. Therefore, a large number of measurements (several hundred) is required to register reliably a low-mass planet with the RV method. At the same time, to measure a small mass of a transit planet, significantly less measurements are sufficient, because the orbital period of such a planet is precisely known from the observations of transits.

4 CONCLUSIONS

The mass distributions obtained earlier for two samples of exoplanets, which were detected by the transit method (A20) and the RV one (I20) and corrected for observational selection effects, somewhat differ. Our analysis has shown that this discrepancy is caused, first, by the fact that different intervals of the orbital period values are used in these samples of exoplanets. The second cause is that the sample of transit exoplanets includes the objects which masses were determined with the TTV method. In the distribution of transit exoplanets which masses are determined only by the RV method, a minimum appears in a range at 0.1 $M_{\rm J}$, which is present in the distribution of RV planets and caused by the hot Neptunian desert.

The agreement is achieved when exoplanets only with short orbital periods (from 1 to 100 d) and masses larger than 0.02 $M_{\rm J}$ are considered both for the distributions built from observational data and those corrected for the observational selection. When converting the distribution of transit exoplanets versus masses to that versus projective masses, this agreement becomes better.

ACKNOWLEDGEMENTS

We are grateful to J.L. Bertaux for valuable comments and to E.V. Petrova for translating the paper into English. The study was supported by the Government and the Ministry of Education and Science of Russia [grant number 075-15-2020-780 (N13.1902.21.0039)].

In this paper, we used the NASA Exoplanet Archive, which is operated by the California Institute of Technology, under contract with the National Aeronautics and Space Administration under the Exoplanet Exploration Program.

DATA AVAILABILITY

The data underlying this article will be shared on request to the corresponding author.

REFERENCES

Ananyeva V. I., Ivanova A. E., Venkstern A. A., Shashkova I. A., Yudaev A. V., Tavrov A. V., Korablev O. I., Bertaux J.-L., 2020, Icarus, 346, 113773
Emsenhuber A., Mordasini C., Burn R., Alibert Y., Benz W., Asphaug E., 2020 A&A(Forthcoming article)
Fortney J. J., Marley M. S., Barnes J. W., 2007, AJ, 659, 1661
Hadden S., Lithwick Y., 2013, AJ, 787, 80
Ho S., Turner E. L., 2011, AJ, 739, 26
Ivanova A., Ananyeva V., Venkstern A., Shashkova I., Yudaev A., Tavrov A., Korablev O., Bertaux J.-L., 2019, Astron. Lett., 45, 687
Ivanova A., Yakovlev O. Y., Ananyeva V. I., Shashkova I. A., Tavrov A. V., Bertaux J.-L., 2021, Astron. Lett., 47, 43
Mazeh T., Holczer T., Faigler S., 2016, A&A, 589, 7
NASA Exoplanet Archive, 2021
Petigura E., Howard A., Marcy G., 2013, PNAS, 110, 19273
Winn J., 2011, in Seager S., ed. EXOPLANETS, University of Arizona Press, Tucson, AZ
Yakovlev O. Y., Ananyeva V. I., Ivanova A. E., Tavrov A. V., 2021, Sol. Syst. Res., 55, 200